Scanning Microscopy

Volume 3 | Number 1 Article 12

1-26-1989

Scanning Electron Microscope and X-Ray Diffraction Investigations of Mudrock Fabrics, Textures and Mineralogy

J. M. Huggett
BP Research Centre

Scanning Microscopy, Vol. 3, No. 1, 1989 (Pages 99-109) 0891-7035/89$3.00+.00
Scanning Microscopy International, Chicago (AMF O'Hare), IL 60666 USA

SCANNING ELECTRON MICROSCOPE AND X-RAY DIFFRACTION INVESTIGATIONS OF MUDROCK FABRICS, TEXTURES AND MINERALOGY

J.M. Huggett

BP Research Centre, Chertsey Road,
Sunbury-on-Thames, Middx, TW16 7LN
Phone No.: (0932) 762966

(Received for publication August 4, 1988, and in revised form January 26, 1989)

Abstract

Mudstones from a broad range of depositional environments have been investigated to determine whether fabric, texture or mineralogy may (1) be used to identify the environment of deposition and (2) be correlated with poroperm. The diversity of fabrics and textures reflects features of the detrital mudstone composition, compaction and diagenesis, rather than environment of deposition. Preferred orientation has been disturbed by bioturbation and growth of post-compactional authigenic minerals; these factors have reduced to nil any correlation which may have existed between fabric, measured as the illite orientation ratio (O/R) and environment of deposition.

It is mineralogy rather than fabric or texture which, after compaction, have most influenced the poroperm. Preliminary results suggest that abundant illite/illite-smectite results in higher poroperm than abundant detrital kaolinite.

KEY WORDS: Mudstone, fabric, diagenesis, orientation, ratio, scanning electron microscopy.

Introduction

Previous Work

Much work has been done on the textural and mineralogical composition of unconsolidated fine-grained sediments as related to their physical properties. Athy (1930), Hedberg (1936), Jones (1946) and Weller (1959) made extensive investigations into the compaction of fine-grained sediments. Studies of fissility in shales and other fine-grained sediments have been made by Lewis (1924), Ingram (1953) and others. Kaarsberg (1959) utilized sound-propagation and X-ray analysis in the investigation of mineral composition, particle orientation and interparticle adhesion in natural and artificial fine-grained sediments. White (1961) made laboratory and field observations on the relationship between the environment of deposition of shales and the origin of such internal structures as fissures, slickensides, fissility and syneresis cracks. He also demonstrated a lack of correlation between fissile structure and depth of burial. This was corroborated by Gipson (1966) who showed that clay particle orientation does not increase with depth of burial. Meade (1964) reviewed a large volume of literature relating to the removal of water and rearrangement of particles during the compaction of clayey sediments. He concluded that the experimental evidence suggests that the development of preferred orientation under overburden load would be encouraged by a fabric that has been partly oriented at the onset of compaction, increasing size of clay minerals, decreasing concentration of interstitial electrolyte, decreasing cation valence, decreasing acidity and the presence of organic matter.

Meade (1963) investigated the causes of an "anomalous" positive correlation between depth of burial and porosity. He attempted to isolate the main factors related to the observed correlation by the use of simple and partial correlation. Gipson (1966) studied the relationships between depth, porosity and clay mineral orientation in Pennsylvanian shales.
He found that porosity decreased slightly with depth but this correlation was strongly influenced by illite content and clay mineral orientation. Porosity was found to decrease

with an increase in clay mineral preferred orientation and an increase in illite content. Ingram (1953) concluded from a study of fissility in a large number of mudrocks that organic matter is the only cementing agent which does not hinder development of fissility and that the latter is independent of clay mineral types present.

Because of the difficulties involved in making detailed textural and petrographical studies of fine-grained sediments most theories regarding such sediments were based on gross-generalizations or indirect evidence from x-ray methods until electron microscopes became available to geologists. O'Brien (1970) used SEM of mudstones fractured perpendicular to bedding and TEM of platinum replicas of fissile plane mudstone surfaces to establish close correlation between clay-flake preferred orientation and fissility. He found randomness of clay flakes to prevail in non-fissile claystones. O'Brien et al. (1980) demonstrated using SEM, that clay fabric may be used in combination with other sedimentary features to distinguish hemipelagic sediments from turbidites. However, Azmon (1981) suggested that deposition of clay into the pore spaces of the unconsolidated silt may introduce a high degree of clay mineral preferred orientation and increase the proportion of clay, which would make the facies identification less simple and possibly unreliable. Using X-radiography and SEM, O'Brien (1987) investigated the effects of bioturbation on the fabric of fifty different shales. He distinguished bioturbated fabrics from those formed from lithified, flocculated clay by the absence of the stepped particle domains or stepped cardhouse fabric characteristic of the latter.

Phakey et al. (1972) used TEM to examine the fine-grained phyllosilicates in ultrathin rock sections of a siderite concretion and a slate. Using selected area diffraction they obtained 001 diffraction patterns of individual particles. They were able to identify 7, 10 and 14Å structures *in situ* in the rock sections. This combination of detailed, high resolution, textural information with structural identification of individual particles affords a powerful method for the investigation of mudstones. However, most of the geological TEM work to date has either been deformation/metamorphic studies (Knipe and White 1977, Bell et al. 1986, Brodie, 1980) or more rarely studies of sandstones (Huggett and White, 1982; Whittle, 1986).

A more recent addition to the range of techniques available for the study of mudstone fabric is the use of SEM in backscattered electron imaging (BSEI) mode to examine polished thin sections. Detailed diagenetic sequences in mudstones which had previously only been inferred in outline from XRD data have been identified (Krinsley et al. 1983; Pye et al. 1986; White et al. 1984). In a BSEI study of interbedded mudstones and sandstones Huggett (1986) demonstrated the potential of this technique for mass balance calculations based on diagenetic import/export between the two lithologies.

Present Study

The literature reviewed above demonstrates that a lack of direct observations has in many instances limited the interpretation of mudstone data. Mudstone petrography has lagged far behind sandstone petrography due to the lack of sufficiently high resolution techniques. Sandstone petrography can usually be adequately performed using thin-sections and an SEM. The advent of back-scattered electron imaging (BSEI) in the SEM, together with recognition of the advantages of using TEM for high resolution / magnification petrography has meant indirect methods (specifically XRD) are no longer the only ones available for the study of mudstone petrography. It is now possible to make detailed textural observations which promise a better understanding of mudstone diagenesis, mineralogy, fabric (defined as particle orientation), and texture (defined as the arrangement, size, and shape of particles). Presented in this paper are the results of a pilot study of mudstone fabrics. SEM was used principally to observe fabrics, whilst XRD was used to measure the degree of preferred orientation and record the mineralogical composition. It is intended that the data herein should point to the need for further work, rather than that inferences should be based upon the data.

Materials and Methods

Samples were collected from four broad depositional environments: deep marine, shallow marine, alluvial, arid intertidal/supratidal. Particular attention was paid to sampling the major North Sea source rock, the deep marine Kimmeridge Clay Formation (Jurassic) and its lateral equivalent the Nesna Formation in the Haltenbanken area of offshore Norway. 1 sample of the shallow water facies of the Kimmeridge Clay Formation was collected from outcrop in Dorset (the Blackstone Oil Shale). A total of twenty-two samples were selected to cover a range of lithological types, i.e., organic content, style of bedding, fissility, grain size, mineralogy, etc. Stratigraphic data and depositional environment are listed for all samples in Table 1.

Other samples were obtained from the Permian Lower Leman sandstone Formation which is a red bed sequence, predominantly sandstone with mudstone interbeds, the Silverpit Formation which is a Permian red mudstone underlying the Lower Leman sandstone, the Lias from onshore Dorset, the Cretaceous mudstones from the Western Approaches off Ireland, the Triassic Sherwood Sandstone from offshore Dorset UK, the Palaeocene Andrew Formation Tuff member from the North Sea, the Triassic Marnock Sandstone from the North Sea, the Coal Measures (Pennsylvanian) from on and offshore UK, and the Cretaceous Calumbri member of the Piacabucu formation from Brazil.

XRD Fabric Orientation Ratio

Several methods for measuring fabric by XRD have been described in the literature. The

Table 1. Sample Data

SAMPLE	DEPTH(m)	AGE	FORMATION	LOCATION	DEPOSITIONAL ENVIRONMENT
			Deep Marine		
Piacabucu Fm	2354.2	Palaeocene	Piacabucu	Brazil	Hemipelagic
KCF2	2478.6	Jurassic	Kimmeridge Clay	North Sea	Distal Turbidite/Hemipelagic
KCF3	4657.25	"	"	"	"
KCF4	3229.6	"	"	"	"
KCF5	3386	"	"	"	"
KCF6	3393.9	"	"	"	"
KCF7	3745.35	"	"	"	"
Nesna Fm.1	1620.0	"	Nesna	"	"
Nesna Fm.2	1638.0	"	Nesna	"	"
Tuff Mbr. Andrew Fm.	2207.02	"	Andrew	"	Submarine Fan
			Shallow Marine/Tidal		
Blackstone Oil Shale	Outcrop	Jurassic	Kimmeridge Clay	Dorset, UK	Unbioturbated v.Shallow Marine
Lias	Outcrop	"	Lias	Dorset, UK	Sub-Wave Base Shallow Marine
Undiffer. E. Cretac.	989.6	Cretaceous	?	Western Approaches UKCS	Bioturbated Shallow Marine
KCF-1	2768.62	Jurassic	Kimmeridge Clay	Porcupine Basin Offshore Ireland	Lagoonal, Tidal Flat
			Arid/Intertidal/Supradital		
Silverpit Fm.	3820.6	Permian	Silverpit	North Sea	Muddy Sabkha
Sherwood Sst.Mbr.	5345.3	Triassic	Sherwood	"	Sabkha/playa Lake
L.Leman Sst.Fm.1	3167.05	Permian	L.Leman	"	Muddy Sabkha
L.Leman Sst.Fm.2	3120.65	"	"	"	Playa Lake?
L.Leman Sst.Fm.3	3187.85	"	"	"	Muddy Sabkha
			Alluvial		
Marnock Sst.	4726.2	Triassic	Marnock	North Sea	Overbank Mudstone
Coal Measures 1	1405.0	Carboniferous	Coal Measures (Pennsylvanian)	"	Overbank Siltstone
Coal Measures 2	3847.0	Carboniferous	Coal Measures (Pennsylvanian)	"	Floodplain Lake

method of Gipson (1966) was selected for this study because it is reliable and gives reproducible results. Measurements were made on 2 mm thick 20 mm² slices of rock cut parallel to and perpendicular to bedding. The orientation ratio (O/R) is calculated by the following ratio of illite peaks;

$$O/R = \frac{\dfrac{A_{002}}{A_{020}}}{\dfrac{B_{002} + C_{002}}{B_{020} + C_{020}}} \qquad (1)$$

Where A_{002} and A_{020} are the peak heights of the illite 002 and 020 reflections for the horizontal surface and B_{002}, B_{020}, C_{002} and C_{020} are the corresponding averages for the 2 vertical surfaces. In the absence of illite another clay mineral could be used but the ratio would not be exactly comparable; fortunately illite was only absent from one sample.

Ratios greater than 1.0 indicate progressively greater orientation, parallel to bedding. The O/R is independent of the proportion of illite in a rock: however, it will be influenced by the illite crystallinity. Because the illite measured in this study is largely detrital and from low temperature grade rocks, this is probably unimportant in this instance.

Measurements were made with a Siemens D500 x-ray diffractometer, using Ni filtered Cu Kα radiation.

SEM analysis of rock slices

SEM was carried out using a JEOL 733 Superprobe (in the geology department, Imperial College, London) a CAMSCAN Series 4 and an ISI 100A scanning electron microscope.

The samples used for SEM were either the A or B rock slice prepared for the orientation ratio measurement described above (i.e. cut perpendicular to bedding). After mounting on an SEM stub the face to be examined was cleaned of loose particles by repeated stripping with ordinary sellotape, and then carbon coated.

This technique provides an ideal means of examining mudstone fabric in 3D and making qualitative porosity measurements. It has the advantage over thin section techniques that soft clays are not smeared by grinding or polishing. X-ray analysis is also possible, but with the geometric and software limitations of the SEMs used analyses are at best semi-quantitative. Secondary electron imaging (SEI) mode of surface examination was mostly used. However, for samples with minerals of a wide range of mean atomic number, combined SEI and backscattered

Table 2A. Bulk probe analyses

Sample	Na_2O	MgO	Al_2O_3	SiO_4	K_2O	CaO	SO_4	MnO	TiO_2	FeO/Fe_2O_3	Total	O/R
PIACABUCA FM.	1.746	0.444	19.560	58.216	3.213	0.638	0.462	0.114	0.336	1.769	86.497	15.98
KCF2	0.345	0.202	32.465	40.030	0.282	0.082	0.744	-	4.099	0.600	78.849	-
KCF7	0.164	0.315	7.981	46.697	1.738	0.201	6.311	0.032	0.273	2.529	66.242	9.82
KCF3	0.486	1.323	17.851	43.572	3.920	0.035	0.455	-	0.195	2.131	69.969	5.33
KCF4	0.712	0.434	17.173	42.081	1.937	0.147	9.145	0.030	0.761	4.099	76.518	11.6
KCF5	0.405	0.409	12.446	35.530	1.324	0.185	13.213	-	0.373	5.377	69.262	13.5
KCF6	0.663	0.475	12.899	39.830	1.400	0.091	4.730	0.011	0.437	2.319	62.855	1.68
Lias West Cliff*	0.276	1.724	8.419	22.596	1.729	21.674	1.365	0.022	0.041	1.816	59.663	2.76
E. Cretaceous§	3.327	1.205	17.865	45.814	2.664	0.176	0.679	0.028	0.597	3.090	74.446	1.86
KCF1	0.649	0.838	29.646	43.172	3.565	0.288	0.406	-	0.902	4.092	83.599	1.6
Silverpit Fm.	3.819	0.382	24.084	49.362	5.468	0.068	0.133	-	0.949	8.600	92.864	4.32
L.Leman Sst Fm.2	0.666	1.129	20.645	56.910	5.981	0.142	0.092	-	0.982	6.913	93.461	8.46
U.Sherwood Sst mbr	1.889	2.924	14.215	45.391	5.962	4.732	0.521	0.239	0.439	4.808	81.120	1.61
L.Leman Sst Fm.1	0.544	1.082	17.623	61.264	4.826	0.171	0.111	0.048	0.914	5.835	92.417	8.46
L.Leman Sst Fm.3	0.497	1.095	21.618	54.894	6.015	0.463	0.165	0.069	0.692	5.597	91.105	1.31
Andrew Fm.Tuff mbr.	0.455	0.588	24.743	54.762	2.982	0.329	0.383	0.137	1.255	2.038	87.672	2.05
Nesna Fm.1	1.471	1.317	12.862	53.226	1.153	0.315	5.588	-	0.275	1.63	77.922	5.94
Nesna Fm.2	0.876	1.923	21.007	47.014	1.286	2.463	8.358	0.064	0.379	2.094	85.742	6.29
Marnock Sst. Fm.	0.936	2.050	23.033	47.029	6.255	1.670	0.248	0.072	0.631	4.094	86.017	1.79
Coal Measures 1	0.354	2.536	30.987	37.950	3.826	0.096	0.237	0.277	1.062	11.657	88.982	-
Coal Measures 2	3.533	1.324	20.427	56.497	4.150	0.204	0.282	-	0.770	3.558	91.103	2.58
Blackstone Oil Shale	0.359	0.453	4.289	7.910	0.650	4.525	14.004	-	0.084	0.952	33.227	44.4

*Dorset, UK. §Western Approaches UKCS. Depths in meters. N.B. Only one analysis was made per sample.

electron imaging (BSEI) or just BSEI were used. In a BSEI image, minerals with a high mean atomic number are readily identified because they appear white against a background of grey tones; this proved particularly useful in recognising pyrite, hematite and chlorite.

SEM analysis of polished thin sections

Polished thin sections cut perpendicular to bedding were examined solely in BSEI for the purpose of observing textures and fabrics and obtaining quantitative probe analyses of individual grains, domains of clay particles (too small to analyse individually with a probe) and bulk sample chemistry.

Results

Mineralogy

A total of 19 minerals were identified in the sample suite, covering a range of minerals comparable with that found in most clastic rocks (Folk, 1968; Pettijohn et al., 1972). The relative proportions of the minerals measured by XRD varied widely, e.g., quartz 9-65%, illite 0-84%, kaolinite 0-33% (Table 2).

The proportion of quartz is closely related to the grain size; mudstones with silt laminae (e.g., the Calumbri member of the Piacabucu formation: 65% quartz by XRD) clearly contain more quartz than do claystones (e.g. the Silverpit Formation: 18% quartz by XRD). However, the proportion of grains estimated visually from SEM examination is invariably less than the total quartz plus feldspar estimated by XRD, indicating the presence of clay-grade quartz and feldspar. The larger the discrepancy, the more clay grade quartz and feldspar may be assumed to be present.

Table 2B - Semi-quantitative XRD analysis of the Alluvial Mudstones.

Sample	Marnock Sst.	Coal Measures 1	Coal Measures 2
Quartz	15	37	13
K Feldspar	-	-	2
Albite	5	3	-
Muscovite	T	T	T
Chlorite	4	2	11
Illite	49	42	67
Ankerite/Dolomite	24	T	1
Siderite	-	2	T
Orientation Ratio	1.79	N/D	2.58

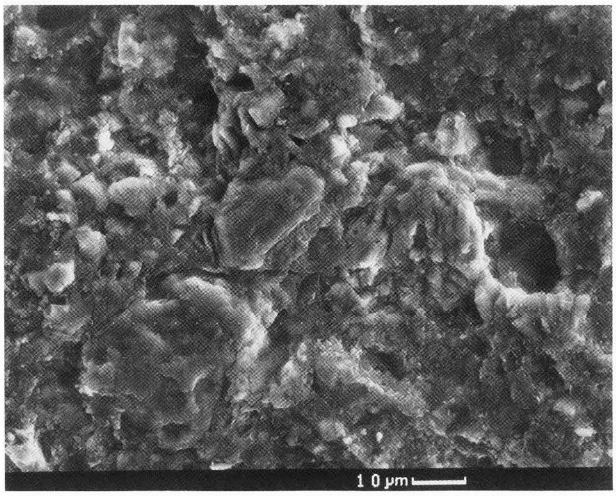

Figure 1. SEI, Lias mudstone (Lower Jurassic) from Lyme Regis, Dorset, UK. Detrital calcite with negligible porosity. O/R = 2.76.

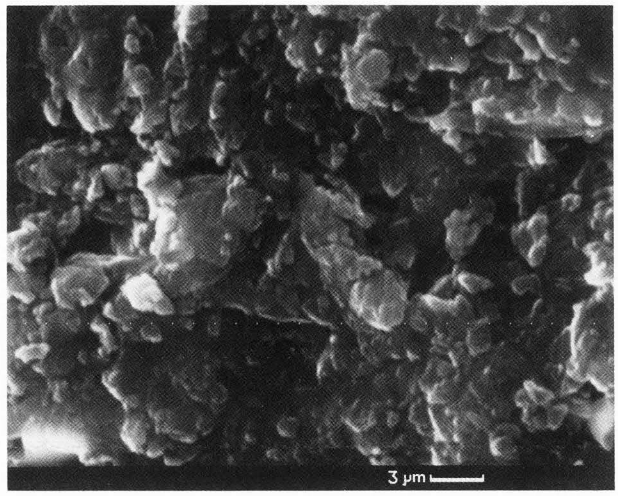

Figure 2. SEI, mudstone from the Piacabucu Formation (Cretaceous, Brazil). Fine-grained detrital kaolinite with low interparticle porosity dominates the clay mineralogy. O/R = 15.98.

Detrital minerals detected are quartz (including minor chert and polycrystalline quartz rock fragments), albite, K-feldspar, muscovite, chlorite, illite, illite-smectite, kaolinite and rare calcite, biotite, ilmenite, rutile and apatite. Authigenic minerals detected are calcite, ankerite, dolomite, siderite, pyrite, hematite, kaolinite, rare quartz, illite, halite, rutile and a CrFeTi oxide (one observation only). Of these the ankerite, dolomite, siderite, pyrite, hematite, halite and CrFeTi oxide were entirely authigenic.

__Textures__

Most of the silty samples come from parallel or cross-laminated units. A few samples were bioturbated (recognised by the circular view in cross-section of disturbed sediment within undisturbed sediment) or slumped. Except for silt/sand laminae, where packstone texture predominates, these mudstones all have a wackestone texture. The highest proportion of grains (throughout the text 'grains' is used to indicate particles of silt size or larger) occurs in the samples with silt/sand domains. In the Kimmeridge Clay the proportion of grains estimated from micrographs is highly variable: 5-40%. In the other samples (without silt/sand domains the proportion of grains was estimated at 5-15%, with one value of 25% for the sample from the Triassic Upper Sherwood Sandstone member (Dorset, UK).

The resolution of the microscopes used was insufficient to examine textures in the claystones, i.e., rocks consisting entirely of clay-size particles.

__Poroperm__

Porosity is generally evenly distributed, with visible (in the SEM) pore sizes up to 1 x 3 µm. Compaction has been responsible for most porosity and permeability loss whereas authigenic cements have relatively little effect, tending to be very finely crystalline and finely dispersed (e.g., pyrite and hematite). However, where large volumes of authigenic dolomite or calcite occur the observed porosity, and presumably permeability, is extremely low. Where there are quartz or other grains larger than clay particles or a disturbed fabric, compaction has been less effective, with the result that the pores are larger. The largest pores (mostly <5 µm, but up to 30 µm) are associated with feldspar dissolution. The smallest pores occur where calcite or detrital kaolinite are abundant (Figs. 1 and 2). Pores are also more equant where calcite and detrital kaolinite are abundant. Samples dominated by clays other than kaolinite develop textures with predominantly oblate pores.

__Fabric Measurement__

Gipson (1966) stated that an orientation ratio of 1.0 indicates preferred orientation; this study shows that such a preferred orientation is not apparent from SEM images until O/R equals approximately 4 (O/R measurements are listed in Table 2 and for each Figure).

There is some correlation evident between high O/R measurements and quiet water clay sedimentation, but this is reduced by diagenesis, through growth of authigenic cements. Where a sample has domains of random and preferred orientation the O/R is a mean value because it is measured over the whole sample. There is no trend towards increasing O/R with depth (which is believed to be close to maximum burial depth for all samples) indicating that factors other than compaction are important (Fig. 3). As a result there is no correlation between % coarse grains and O/R (Fig. 4).

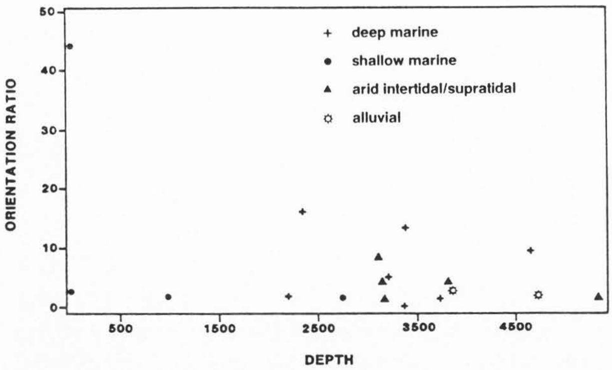

Figure 3. Plot of orientation ratio versus depth.

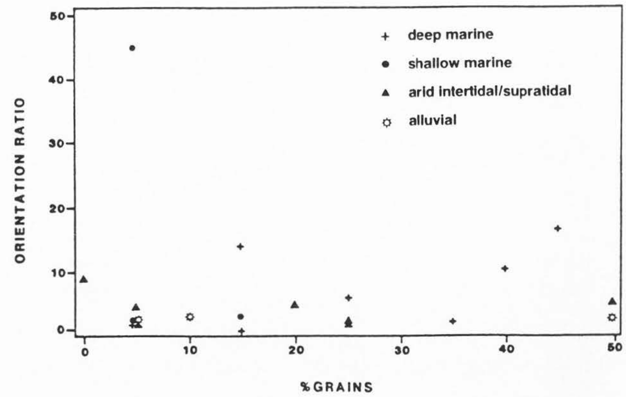

Figure 4. Plot of orientation ratio versus percentage grains.

Discussion

Importance of Mineralogy, Texture and Fabric as Indicators of Depositional Environment

Texture and Mineralogy Bimodal detrital grain size distribution was observed in samples from muddy sabkha (Fig. 5) and alluvial floodplain environments only. Size, sorting (other than bimodal), roundness, sphericity, fracturing, pressure solution and leaching do not correlate with any particular depositional environment or mechanisms for the samples studied.

Quartz is present in all samples and its distribution does not reflect environment of deposition whether measured as total quartz (by XRD) or total visible quartz grains (estimated from polished thin sections). The size of the grains is rarely greater than 60 μm, but may be up to 300 μm. In many samples the discrepancy between % quartz and % grains implies that as much as 25% of the quartz is clay grade, ie, too fine-grained to observe as grains (Fig. 6).

Authigenic carbonates occur in all depositional environment samples, with calcite being most abundant in the shallow marine, and dolomite in the alluvial and arid intertidal/supratidal environments.

Ankerite and dolomite occur as euhedral rhombic crystals replacing, or intergrown with the matrix (Fig. 7). Siderite and authigenic calcite generally form micritic cement (Fig. 8) replacing matrix, or as small scattered rhombs. Calcite more rarely occurs as poikilotopic crystals and siderite as wispy blades (Fig. 9). Detrital calcite generally occurs as fossil debris in particular, coccoliths; it was only observed in the marine environments (Fig. 10).

Pyrite mostly occurs as framboids (<25 μm) and finely dispersed sub-micron size particles (Fig. 11). Pyrite also occurs as large euhedral crystals (Fig. 11), particularly when replacing detrital quartz or feldspar grains. Pyrite only occurs in the marine mudstones, presumably reflecting the relative abundance of sulphate in marine waters. In the Nesna and Kimmeridge Clay Formations pyrite has replaced fossil fragments (Fig. 10).

Hematite occurs only in the arid environments where suitable oxidising conditions can occur. Hematite generally forms finely disseminated sub-micron sized particles (Fig. 12): less often it replaces grains.

Detrital kaolinite occurs as very-fine grained (<1 μm) particles in samples from all environments except the arid where it is absent (Fig. 2). In the four Kimmeridge Clay Formation samples from UKCS block 211/12A, (KCF3, 4, 5 and 6) authigenic kaolinite has partially replaced muscovite particles to form kaolinite/muscovite

Figure 5. BSEI, bimodal grain size distribution in a mudstone from a muddy sabkha interval in the Permian Lower Leman Sandstone Formation, North Sea. Fine-medium grains occur in the top left hand and bottom right hand sectors; very fine-fine grains in the middle. Q = quartz, H = hematite. O/R = 1.34.

Figure 6. BSEI, tuff member of the Paleocene Andrew Formation, North Sea. The discrepancy between the percentage quartz (XRD) and the percentage grains implies that as much as 25% of the quartz may be of clay grade. In this instance the quartz may be the product of volcanic glass alteration. O/R = 2.05.

Figure 7. BSEI, euhedral rhombs of authigenic dolomite (D) in the Triassic Upper Sherwood Sandstone Member, Dorset, UK. O/R = 1.61.

Figure 8. BSEI, sub-hedral rhombs of authigenic calcite (c) in the Blackstone oil shale, Jurassic Kimmeridge Clay Formation, Dorset, UK. O/R = 44.4.

Figure 9. BSEI, wispy blades of authigenic siderite (s) in undifferentiated Early Cretaceous mudstone, Porcupine Basin, offshore Ireland. O/R = 1.86.

Figure 10. BSEI, fossil debris in the Jurassic Blackstone oil shale, with intra-particle calcite cementation (c). The fossil fragment itself has been replaced by pyrite (P). The black patches are organic matter, most of the matrix is calcite with some quartz and illite. O/R = 44.4.

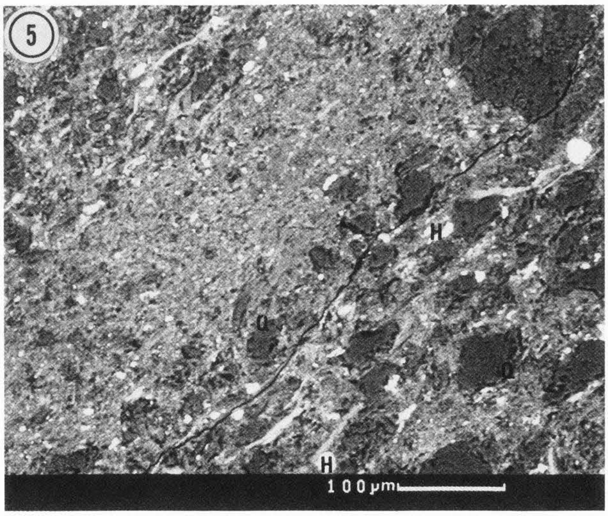
5
H
Q
Q
H
100 μm

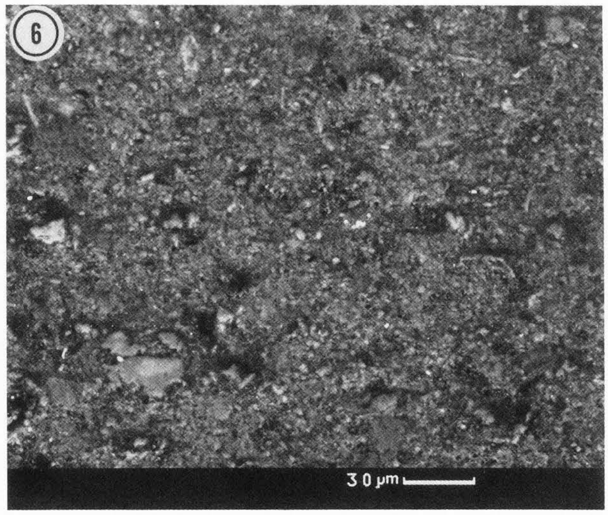
6
30 μm

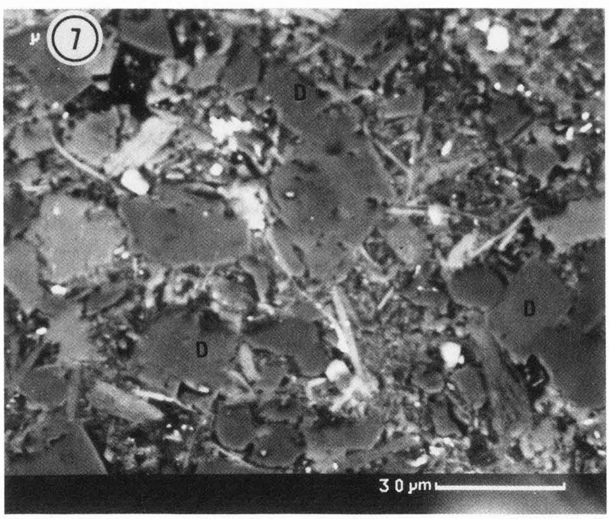
7
D
D
D
30 μm

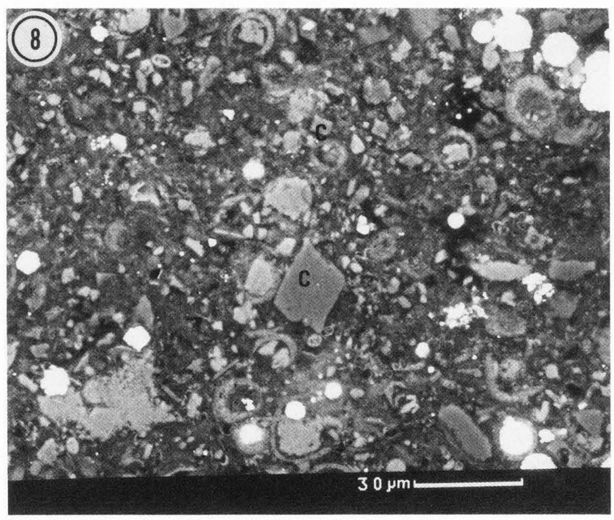
8
C
C
30 μm

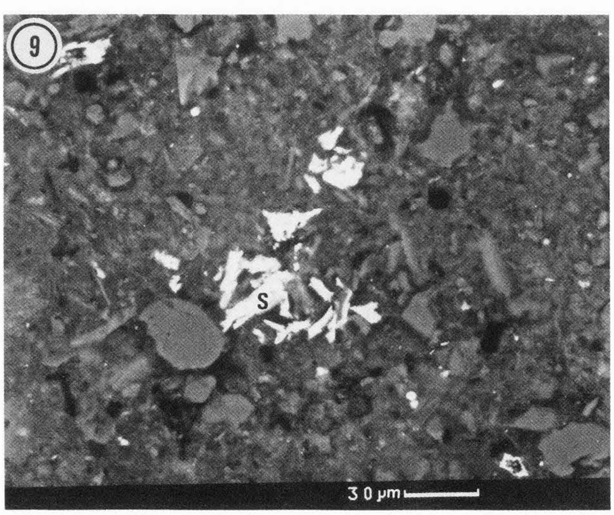
9
S
30 μm

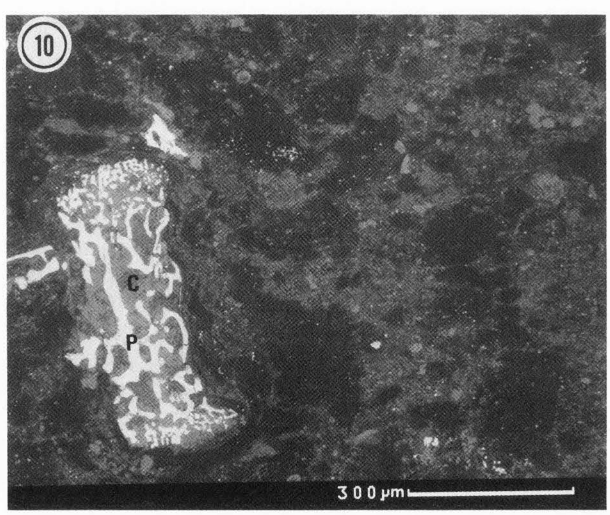
10
C
P
300 μm

stacks (Fig. 11). More samples from a range of depositional/diagenetic environments would be required to determine the factors controlling this reaction.

Illite is the most widespread and abundant clay in the studied sample suite and is thus not a useful indicator of depositional environment. This observation may be explained by the high concentration of micas in many rock types, the widespread abundance of illite in many soils, and its relative resistance to chemical weathering (Jackson et al., 1948; Reiche, 1950). Only by XRD could illite be distinguished from illite-smectite. It occurs as flakes up to 10 μm in diameter (Fig. 13). Authigenic illite is difficult to identify in mudstones, particularly if it replaces other clays, e.g. illite-smectite or smectite. However, it was occasionally observed rimming mica grains and as small wispy growths on grains (Fig. 14).

The only fully expandable clay found was K bentonite in the Nesna Formation, it has been suggested that this is a diagentic alteration of a volcanic ash fall deposit (pers. comm. C. Curtis, Manchester University).

Alkali feldspars occur in all environments, and in virtually all samples, though never exceeding 5% of the rock. Distribution is probably related to provenance factors rather than depositional environment. Feldspar grains may be up to 300 μm, but are mostly <60 μm. K-feldspar in particular is often slightly leached. Leaching is likely to be controlled by the amount of contact with fluids having low K+ and Na+ concentrations. In the Nesna Formation *in situ* replacement of feldspar by clay has occurred (probably K bentonite) (Fig. 15). No authigenic feldspars were observed.

Detrital mica distribution shows no relationship to depositional environment either. Muscovite was observed in all but three samples. It is generally chemically unaltered, it is rarely leached showing only splayed terminations, except in Kimmeridge Clay samples 3 to 6 where it is intergrown with replacive kaolinite. Biotite was only observed in a few samples. Its scarcity reflects either provenance or more probably its instability, rather than environmental control on its distribution. However, detrital chlorite grains and clay-grade chlorite particles are almost completely restricted to the arid and alluvial environments. It may therefore be possible to use chlorite as an indication of the range of environments possible for a given mudrock sample.

Organic matter was observed in samples from all environments except the arid it is identified in BSE images as the black amorphous material, often with fine inclusions. It is most abundant in the Kimmeridge Clay, with visually estimated values of 50% for the Blackstone Oil Shale. The organic particles vary considerably in shape from large (up to 100 μm) tabular, braided or skeletal (Fig. 11), to fine irregular/platey clay/silt size particles (Fig. 9). In the Blackstone Oil Shale, the organic particles occur as 30-300 mm pods in which grains and matrix float (Fig. 10).

Figure 11. BSEI, pyrite framboids (F) and single euhedral crystals (P) in the Jurassic Kimmeridge Clay Formation, North Sea. Arrowed, is kaolinite (dark grey) which has partially replaced muscovite (light grey). O/R = 11.6.

Figure 12. BSEI, finely disseminated Haematite (H), Permian Lower Leman Sandstone Formation mudstone, North Sea. The large white grain (arrowed) is a TiCrFe oxide. O/R = 8.46.

Figure 13. SEI, detrital illite from the Permian Lower Leman Sandstone Formation, North Sea. O/R = 8.46.

Figure 14. SEI, detrital illite/ illite-smectite with wispy growths of authigenic illite (?), from an undifferentiated Early Cretaceous Mudstone, Porcupine Basin, Offshore Ireland. 3 pores are arrowed. O/R = 1.86.

Figure 15. BSEI, replacement of feldspar (arrowed) by clay, probably k-bentonite, in the Jurassic Nesna Formation, offshore Norway, Bar = 30 micrometers. O/R = 6.29.

Figure 16. BSEI, pyrite framboids (white) in the Jurassic Kimmeridge Clay Formation, North Sea. Bar = 30 micrometers. O/R = 11.6.

Halite crystals were only observed in the arid sabkha mudstone sample from the Silverpit Formation. No gypsum or anhydrite is associated with halite. Rutile occurs as fine rods and pseudomorphous replacement of grains (probably ilmenite) in samples from all environments. In Kimmeridge Clay sample 2 the bulk EDS analysis indicated 4% Ti content. For most samples the figure is 0.5-1%. The rutile is a mixture of ragged (detrital?) and equant (authigenic?). In the sample with 4% it is mostly delicate authigenic rod-shaped crystals. In addition to replacing illmenite authigenic rutile may have formed from Ti released by biotite alteration to illite.

<u>Fabric</u>

A well-defined preferred orientation indicates undisturbed clay sedimentation without subsequent slumping, bioturbation or displacive authigenic mineral growth. Within the present sample suite, it is not possible to use fabric as a more detailed guide to environment of deposition. Moreover any fabric variations due to flocculation of clay prior to deposition, which may have been present, appear to have been removed during compaction: hence any data which might be gleaned regarding water salinity has apparently been lost. For example the O/Rs for the fresh water mudstones vary from 1.79 to 2.58 (low), whilst those for the arid (saline) environment mudstones vary from 1.31 (low) to 8.46 (high).

<u>Importance of texture and fabric as controls on sealing migration and expulsion mechanisms/ efficiency</u>

The detrital kaolinite observed in this study was very fine-grained (<1 μm) and tightly compacted, resulting in low visible porosity.

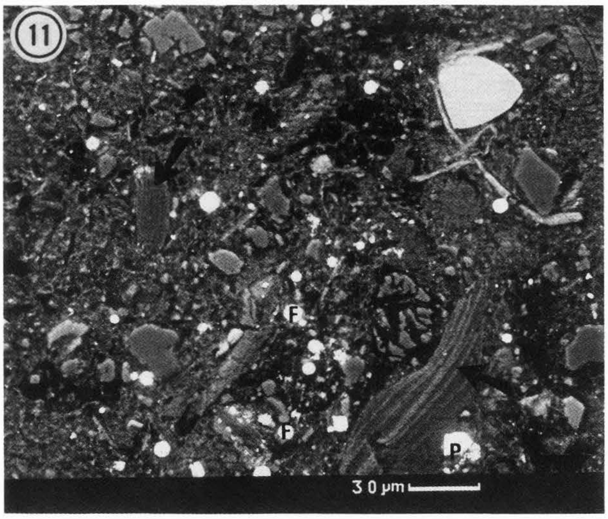
11
F
F
P
30 µm

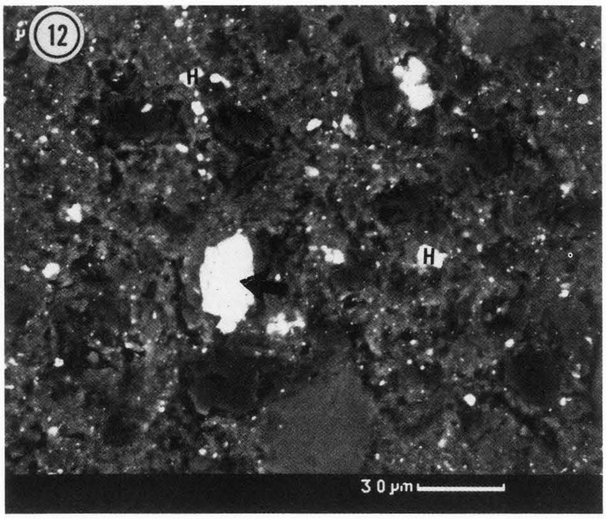
12
H
H
30 µm

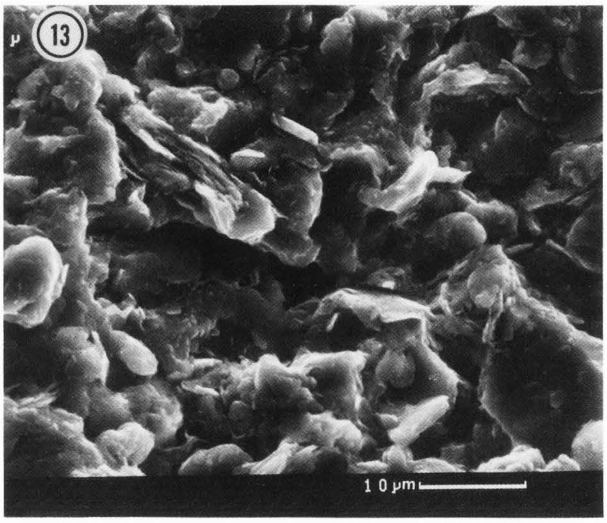
13
10 µm

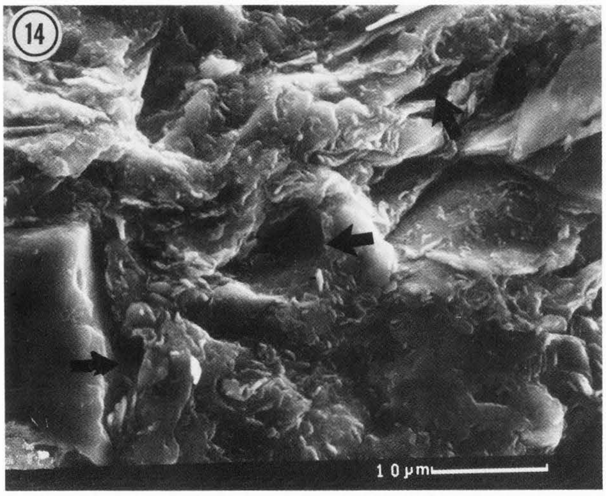
14
10 µm

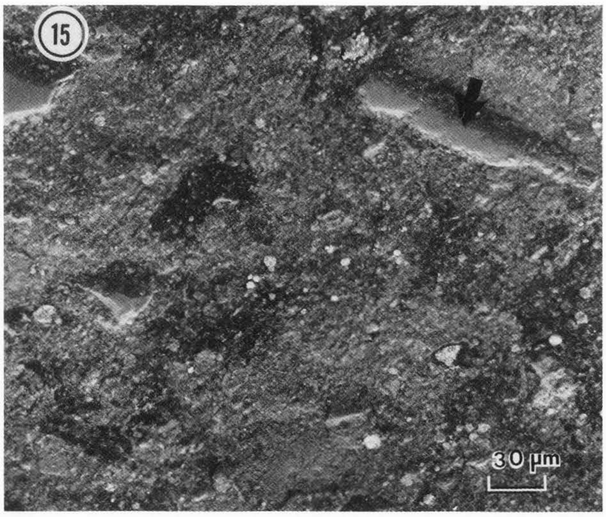
15
30 µm

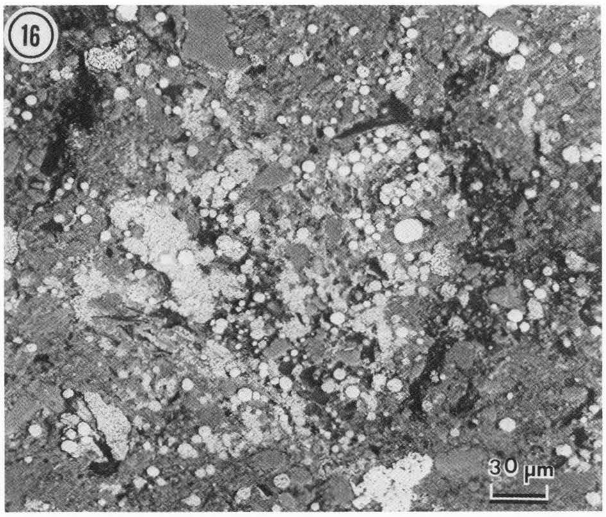
16
30 µm

From observations made during this study it seems that possibly as little as 10% <1 μm size detrital kaolinite can significantly affect mudstone porosity and permeability (Fig. 2). In most rocks containing abundant very fine-grained kaolinite pores tend to be rounded but not necessarily smaller than the oblate pores seen in illitic mudstones. Whether this is significant for hydrocarbon sealing and expulsion mechanisms/efficiency hinges on the pore connectivity and also the distribution of organic matter. Qualitative estimates from SEM observation suggest that the illitic mudstones have greater pore connectivity than the kaolinitic ones and may therefore be more efficient at expelling hydrocarbons, but possibly less effective as seals. However, clay matrix porosity and permeability is only going to be a major factor in the expulsion of hydrocarbons from (1) lean source rocks where the organic matter, which provides the expulsion route is itself poorly interconnected and the oil globules which form in it cannot readily connect up and move through the pores of the residual organic matter, or (2) where micro cracks are not major migration pathways (McKenzie et al, 1987, 1988).

Clay matrix compacts imperfectly around grains resulting in a concentration of relatively large pores, typically 1 x 5 μm (Fig. 14). In sand/silt domains or laminae this may result in enhanced permeability as well as porosity if the pores are interconnected. Large pores also occur around muscovite flakes and as a result of feldspar dissolution: the latter are generally <5 μm.

Conclusions

Some correlation between fabric and textures and environment of deposition is apparent from this study, but it has been reduced through growth of authigenic minerals. However diagenesis and redistribution reactions are controlled by primary mineralogy, the depositional pore fluid and fluid access after deposition. Hence depositional environment does have an indirect influence on the authigenic minerals which form. Dynamic fluid access is severely limited to fractures and silt/sand laminae once the main phase of compaction is over. This results in diagenetic inhomogeneities, with less import/export reactions occurring in the clay rich domains, particularly where detrital kaolinite is present.

Depths from <1 km to >5 km were sampled but no relationship with preferred orientation or any other fabric/textural criteria was observed. This may be because the samples have a wide scatter in composition and depositional environment/mechanism.

Where bioturbation has occurred there is less preferred orientation than in comparable undisturbed samples. More samples would need to be examined before comment could be made on the effect of bioturbation on pore size or connectivity.

Some mineralogical influence over poroperm was also noted. Detrital kaolinite consists of small ragged particles (<1 μm) which have been so thoroughly compacted that it is difficult to pick them out individually. Illite particles are <5 μm and less thoroughly compacted, resulting in larger pores (typically 1 x 3 μm) and possibly better pore connectivity than in kaolinite-rich mudstone (pores typically <1 μm). This implies that kaolinite may result in better seal capacity, but possibly poorer source-rock expulsion efficiency than illite.

Acknowledgements

I am grateful to BP International Limited for permission to publish this work, and to the Geology Department at Imperial College, London for use of their JEOL 733 Superprobe SEM.

References

Athy LF (1930) Density porosity and compaction of sediments: Am. Assoc. Petroleum Geologists Bull. 14, 1-35.

Azmon E (1981) Use of clay fabric to distinguish turbidites from hemipelagic siltstone; Sedimentology 28, 733-735.

Bell IA, Wilson CJL, McLaren AC & Etheridge MA (1986). Kinks in mica: role of dislocations and (001) cleavage: Tectonophysics 127, 49-66.

Brodie KH (1980) Variations in mineral chemistry across a shear zone in phlogopite peridotite: J. Struct. Geol. III 2, 265-272.

Folk RL (1968) Petrology of sedimentary rocks. Hemphill's, Austin, Texas, 170pp.

Gipson M (1966) A study of the relations of depth, porosity and clay mineral orientation in Pennsylvanian shales: J. Sed. Pet. 36/4, 888-903.

Hedberg HD (1936) Gravitational compaction of clays and shales: Amer. J. Sci 5th series, 31, 241-287.

Huggett JM & White SH (1982) High voltage electron microscopy of authigenic clay minerals in sandstones: Clays and Clay Minerals 30, 232-236.

Huggett JM (1986) An SEM study of phyllosilicate diagenesis in sandstones and mudstones in the Westphalian Coal Measures using back-scattered electron microscopy: Clay Minerals 21, 603-616.

Ingram RL (1953) Fissility of mudrocks: Geol. Soc. America Bull, 64, 867-878.

Jackson ML, Tyler S, Willis AL, Bowbeau GA & Pennington RP (1948) Weathering sequence of clay-size minerals in soils and sediments. I fundamental generalisations: Jour. Phys. and Colloid. Chemistry 52, 1237-1260.

Jones OT (1946) The compaction of muddy sediments: Geol. Soc. London. Quart. J. 100, 137-160.

Kaarsberg EA (1959) Introductory studies of natural and artificial argillaceous aggregates by sound-propagation and X-ray diffraction methods J. Geology, 67, 447-472.

Knipe RJ & White SH (1977) Microstructural variations of an axial phase cleavage around a fold - a HVEM study: Tectonophysics 39, 355-381.

Krinsley DH, Pye K & Kearsley AT (1983)

Application of backscattered electron microscopy in shale petrology: Geol. Mag. 120, 109-208.

Lewis GV (1924) Fissility of shale and its relation to petroleum: Geol. Soc. America Bull 35, 557-590.

McKenzie AS, Price I, Leythaeuser D, Muller P, Radke M & Schaeter RG (1987) The expulsion of petroleum from Kimmeridge clay source-rocks in the area of the Brae Oil Field, UK Continental Shelf. In: Petroleum Geology of Northwest Europe. Heyden, London, 865-877.

McKenzie AS, Leythaeuser D, Muller P, Quigley TM & Radke M (1988) The movement of hydrocarbons in shales. Nature 6151, 63-65.

Meade RL (1963) Factors influencing pore volume in fine-grained sediments: Sedimentology 2, 235-242.

Meade RL (1964) Removal of water and rearrangement of particles during compaction of clayey sediments - Review: USGS Prof. Paper 497-B, B1-B23.

O'Brien NR (1970) The fabric of shale - an electron microscope study: Sedimentology 15, 229-246.

O'Brien NR (1987) The effects of bioturbation on the fabric of shale: J. Sed. Petrol. 57, 449-455.

O'Brien NR, Nakazawa K & Tokuharshi S (1980) Use of clay fabric to distinguish turbiditic and hemipelagic siltstones and silts: Sedimentology 27, 47-61.

Pettijohn FJ, Potter PE & Siever R (1972) Sand and Sandstone; Springer-Verlag, Berlin, 618pp.

Phakey PP, Curtis CD & Oertel G (1972) Transmission electron microscopy of fine-grained phyllosilicates in ultra-thin rock sections: Clays and Clay Minerals 20, 193-197.

Pye K, Krinsley DH & Burton JH (1986) Diagensis of US Gulf Coast shales; Nature 324, 11 December, 557-559.

Reiche P (1950) A survey of weathering processors and products: Univ. of New Mexico, Publ. in Geology, No. 3, 95p.

Weller JM (1959) Compaction of sediments: Am. Assoc. Petroleum Geologists Bull. 43, 273-310.

White WA (1961) Colloid phenomena in sedimentation of argillaceous rocks: J. Sed. Petrol. 31, 560-570,

White SH, Shaw HF & Huggett JM (1984) The use of back-scattered electron imaging for the petrographic study of Sandstones and Shales: J. Sed. Petrol. 54, 487-494.

Whittle CK (1986) Comparison of sedimentary chlorite compositions by X-ray diffraction and analytical TEM: Clay minerals 21, 937-948.

Discussion with Reviewers

N.R. O'Brien: You observe no trend toward increasing O/R with depth. When, during the accumulation and burial process, do you think the particle orientation in mudrocks developed?
Author: I think it most probable that the particle orientation in mudrocks develops during the first km of burial when compaction is at a maximum and porosity is reduced from 70% to <10%.

D. Krinsley: You state, re alkali feldspars that "Distribution is probably related to provenance factors rather than depositional environment". Perhaps this parameter could be used to indicate provenance; possibly the amount, size and percent of albite in the K feldspars (if present) might be related to provenance. It has been possible to study the distribution of albite in K feldspars with BSEI; it seems to me that this is an obvious thing to do. Would you care to comment?
Author: Provenance studies were outside the scope of this piece of work. BSEI with image analysis would be ideal for studying the distribution of albite in K feldspar.

D. Krinsley: Is there a relation between the amount of detrital chlorite as related to clay grade chlorite in given samples from specific environment?
Author: The relative amounts of larger than clay grade detrital chlorite and clay grade chlorite were not determined.

D. Krinsley: Do organic particle shapes vary systematically with sample porosity, mineralogy, chemistry etc?
Author: This is to be the subject of a further study.

D. Krinsley: Is there a degree of surface roughness beyond which no BSEI contrast is produced?
Author: This was not investigated but very little loss of BSEI contrast was noted between the polished thin sections and the rock slices cut with a saw.

K. Pye: Is it possible to say to what extent the microfabric of your samples has been affected by drying and oxidation since collection?
Author: This is a question I too should like to know the answer to, but having never had the opportunity to examine preserved core of mudstones I am unable to say.